IEEE Access
Multidisciplinary | Rapid Review | Open Access Journal

Received May 30, 2020, accepted June 13, 2020, date of publication June 18, 2020, date of current version July 2, 2020.

Digital Object Identifier 10.1109/ACCESS.2020.3003416

Automatic Positioning and Recognition of Anesthesia Points Based on Ultrasound Image Guidance Technology

HUANQIU LIU[1], FUZHE MA[2], JI LI[1], TINGTING YU[3], AND XINBAI LI[1]

[1]Department of Anesthesiology, The First Hospital of Jilin University, Changchun 130000, China
[2]Department of Nephrology, The First Hospital of Jilin University, Changchun 130000, China
[3]Department of Otolaryngology, Head, and Neck Surgery, The First Hospital of Jilin University, Changchun 130000, China

Corresponding author: Xinbai Li (lixinbai@jlu.edu.cn)

ABSTRACT Local anesthesia has certain harm to the patient, and the wrong position of the anesthesia point may result in poor anesthesia effect. Based on this, this study built an automatic positioning recognition model based on ultrasound image guidance technology. At the same time, this paper combined the actual requirements of anesthesia to establish a wireless positioning system based on ultrasonic infrared, and the system combined ultrasonic propagation characteristics and sensing receiving characteristics. In addition, in the study, this article combined with the state of the anesthesia point to take ultrasound-guided anesthesia. Finally, this paper designed a comparative experiment to study the performance of automatic positioning of anesthesia points based on ultrasound image guidance technology and collected actual data to analyze. Studies have shown that the method proposed in this study has certain clinical effects and can provide theoretical references for subsequent related research.

INDEX TERMS Ultrasound, image, positioning, image guidance, positioning technology.

I. INTRODUCTION

Local infiltration anesthesia is a commonly used anesthetic method in clinic. For a long time, local anesthesia has been widely used in various surgical fields due to its advantages of simple and easy operation, high safety, clear consciousness of patients and little influence on physiological functions of patients. However, local anesthesia has its own unique complications. F For example, when the local anesthetic is injected too fast or the blood vessel is injected to cause excessive blood concentration in the patient, the patient has local anesthetic poisoning, infection, and nerve damage at the local puncture site. In addition, there are some other rare complications such as abdominal wall penetration, intestinal damage and so on. During the operation, it is more likely to damage the tissues and organs around the target nerve, so it is necessary to effectively guide the anesthesia site, improve the anesthetic effect and reduce the physical damage to the patient [1].

In most of the literature, it is proved that the transverse abdominis plane block can improve the postoperative analgesia effect and reduce the total amount of opioids used in the postoperative controlled analgesia pump. McDonnell *et al.* in the study of TABB in intestinal resection showed that the dose of opioids at different observation time points within 24 hours after surgery was significantly reduced [2]. Carney *et al.*'s study confirmed that after the patient was given TABP, the amount of opioid use was significantly reduced after surgery, and the time of the first self-controlled analgesia pump was prolonged [3]. Studies have found that after giving TAB to patients, the time to first press the self-controlled analgesia pump is significantly longer than that of the blank control group. Kanazi *et al.* added epinephrine to 20 ml of 0.375% bupivacaine when given a flattening of the abdominis muscle. The results showed that the time of the first press-controlled analgesia pump was significantly longer than that of the other group of patients who pressed the self-controlled analgesia pump for the first time, which reduced the side effects of the opioids used in the postoperative self-controlled analgesia pump, reduced the nausea and vomiting and sedation score, and improved the patient's satisfaction with postoperative analgesia, and reduced the postoperative visual analogue system score [4]. However, there are also reports in the literature that

The associate editor coordinating the review of this manuscript and approving it for publication was Zhihan Lv.

TABB has no significant effect on improving postoperative pain and analgesia. Griffiths et al found in the study that there was no significant difference in the time between the first press of the controlled analgesia pump, the total dose of opioids, its clinical side effects, and the postoperative visual analogue system scores compared with the blank control group [5]. Belayy et al found that there was no difference in reducing the side effects of opioids and visual analog system scores [6]. In addition, in comparison with epidural analgesia, Kanazi *et al.* pointed out that ultrasound-guided TABP and epidural single-shot opioid analgesia were observed in the 4h visual analogue system scores lower than the TAP group, and the incidence of nausea and vomiting was higher than the TAPB group [7].

At present, there are still differences on the reports of the sense planes of TABP. After 30 minutes, the sensory block plane of laparoscopic gynecological surgery patients was evaluated by acupuncture, and the highest plane reached T10-L1. Therefore, it was considered that the transverse abdominis plane block can only be used for lower abdominal surgery. Hebbafd studied 21 anesthesia planes after ultrasound-guided TABB, and he believed that TABP could only provide navel analgesia [8]. Tran *et al.* performed ultrasound-guided lower abdominal wall TABP and injected fluorescent dyes into 10 cadaveric bodies and found that the fluorescence fuel spread was up to T10, suggesting that the application of abdominal transverse muscle plane block is limited to low abdominal surgery [9]. The results showed that the volunteers had a feeling of weakening in the anterior abdomen, and the results showed that TABP only exerted the maximum effect after 90 minutes, and the effect began to decrease after 4 hours of block operation, and the longest effect lasted until 24 hours after surgery [10].

In many studies, it has been pointed out that local anesthetic injection of the transverse abdominis can block the nerves that innervate the anterior abdominal wall and provide satisfactory postoperative analgesia for patients. Other studies have used ultrasound-guided TAPB for colorectal surgery and found that TABP is effective in reducing pain during and after surgery [11].

In recent years, with the development of science and technology, ultrasound medicine has also developed rapidly. Moreover, the application of ultrasound technology to nerve block makes the entire operation intuitive, safe, and effective, and makes ultrasound-guided nerve block more and more concerned by anesthesiologists [12].

Traditional nerve block methods cannot observe the distribution and spread of local anesthetics. However, when the ultrasound guides the descending nerve block, the anesthesiologist can directly recognize the anatomy of the nerve and its surrounding tissues through ultrasound imaging. Moreover, under the guidance, by placing the puncture needle into the nerve target to block, the action of the needle can be observed in real time, and the injection process and diffusion distribution of the anesthetic can be dynamically observed to ensure the effective injection of the anesthetic. In 1978, LaGrange et al reported the first peripheral nerve block under ultrasound guidance. Since then, LaGrange and colleagues have used Doppler ultrasound probes to identify and locate the subclavian artery during brachial plexus block, resulting in a nerve block success rate of up to 98% [13], and no anesthetic complications have occurred. As early as in the 1980s, foreign scholar Fomag first performed ultrasound examination of the peripheral nerves and muscles of cadaver specimens and compared them with anatomy. Subsequently, domestic scholars also carried out similar research reports [14]. Since the mid-1990s, various types of nerve block under ultrasound guidance, such as sciatic nerve block, femoral nerve block, brachial plexus block, etc., have achieved good neurological blockade. Marhofer believes that effective injection of local anesthetics is the key to the success of peripheral nerve block. That is, after the local anesthetic infiltration is blocked around the nerve, the ultrasound-guided real-time image can accurately inject the local anesthetic solution around the target nerve, thus ensuring the effect of the nerve tissue [15].

At present, many studies have confirmed that compared with the traditional nerve block method, Ultrasound-guided nerve block has the advantages of fast onset, high block success rate, short operation time, less complications, and the amount of local anesthetic is also significantly reduced. Ultrasound technology is becoming more and more widely used in clinical practice, and this technology has accumulated rich clinical experience abroad. In recent years, domestic clinicians have become more and more concerned about this technology, and have been reported with relevant treatment experience, such as celiac plexus block and prostate nerve block in cancer patients. In some hospitals, ultrasound guidance has become a routine way of nerve block. Therefore, based on the ultrasound guidance technology, this study automatically locates the anesthesia point, improves the anesthesia efficiency and reduces the damage of the anesthesia to the patient's body.

II. RESEARCH METHOD

The positioning idea of two-dimensional ultrasonic positioning is to obtain the position information of the positioning target by measuring the propagation time, angle of arrival, phase and other parameters of the ultrasonic wave and using the geometric triangular relationship and operation. The ultrasonic wave is suitable for target positioning in a local range, and the ultrasonic signal emitted by the mobile terminal is usually received by a known fixed point. According to the parameters of the measured ultrasonic signals, the main methods of ultrasonic positioning are TOA (time of arrival) positioning method based on ultrasonic arrival time, AOA (angle of arrival) positioning method based on ultrasonic arrival angle, and R&DOA (range and direction of arrival) positioning method based on signal propagation distance and angle of arrival [16].

The wireless positioning system based on ultrasonic infrared is mainly composed of periodic transmitting

ultrasonic, infrared transmitting end, two signal receiving end, signal processing module, PC and other components. The positioning principle is shown in Fig. 1 [17]. The left and right signal receivers are horizontally placed at the upper left and upper right of the positioning area, and the coordinate positions of the two signal receivers are known, and the distance d between the receivers can be measured or calculated. The left signal receiver A is used to measure the propagation time of the ultrasonic signal from the signal pen to the receiver A and calculate the distance u between the signal pen and the receiver A. Similarly, the distance v [18] between the stylus and the receiver B can be measured and calculated.

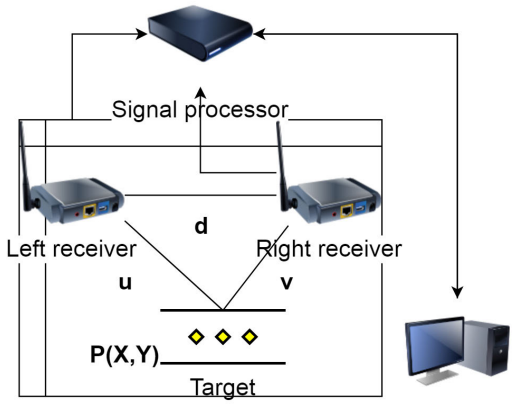

FIGURE 1. Schematic diagram of system positioning.

The propagation time of the ultrasonic signal measured by the signal receivers A and B is τ_1, τ_2. Assuming that the propagation speed of the ultrasonic signal in the air medium is c, the distance u and v between the positioning target and the signal receivers A and B can be calculated as [19].

$$\begin{cases} u = c * \tau_1 \\ v = c * \tau_2 \end{cases} \tag{1}$$

Since the position coordinates of the signal receivers A and B are known as $(x - x_1)^2$, (x_2, y_2), the coordinates of the stylus in the measurement range are (x, y) and according to the triangle Pythagorean theorem, u, v can be obtained as following.

$$\begin{cases} u = \sqrt{(x - x_1)^2 + (y - y_1)^2} \\ v = \sqrt{(x - x_2)^2 + (y - y_2)^2} \end{cases} \tag{2}$$

The coordinates of the positioning target P can be obtained by the formula (1).

$$\begin{cases} x = \dfrac{\left(x_2^2 - x_1^2\right) - (c\tau_2)^2 + (c\tau_1)^2}{2\,(x_2 - x_1)} \\ y = y_1 + \sqrt{(c\tau_1)^2 + (x - x_1)^2} \end{cases} \tag{3}$$

According to the coordinate formula of the positioning target position, since the ultrasonic velocity c is known, the acquisition of the position coordinates is only related to the ultrasonic propagation time, that is, the signal delays τ_1 and τ_2.

In order to achieve high-precision positioning of the system, the most critical problem is the ability to accurately extract the signal delays τ_1, τ_2. There are many ways to realize signal delay information extraction. This system uses the method of ultrasonic and infrared joint positioning, as shown in Fig. 2 [20].

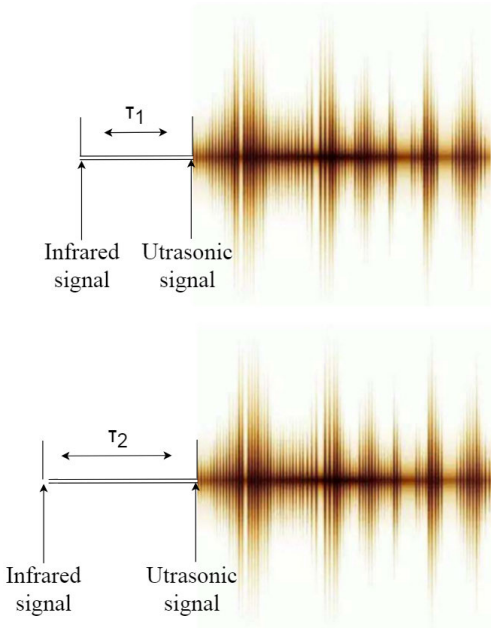

FIGURE 2. Schematic diagram of time delay of two ultrasonic signals.

While the periodicity of the target is being located, the ultrasonic and infrared signals are transmitted. The speed of the infrared signal is 3*108 m/s, and the speed of the ultrasonic signal in the air medium is 340 m/s (affected by the air temperature). The speed of the ultrasound is very low relative to the speed of light. The propagation time of the infrared signal in the range of 1m is negligible. The time when the receiver receives the infrared signal is taken as the start time of the ultrasonic wave propagation, and the ultrasonic signal delay is the time difference between the infrared signal received by the receiver and the ultrasonic signal, that is, τ_1, τ_2 [21].

Through the error analysis of the TOA positioning method used in the positioning system, it can be known that the temperature accuracy of the ultrasonic signal wave speed can ensure the positioning accuracy of the system as long as the measurement accuracy of the left and right ultrasonic delays can be ensured. In order to extract the precise ultrasonic delay, after the ultrasonic signal is acquired by the signal processor, the ultrasonic signal time delay extraction algorithm is designed to accurately determine the ultrasonic arrival time according to the ultrasonic waveform characteristics.

Since the signal transmitting module is battery powered, this part of the circuit needs to provide a stable 3.3V voltage for the microcontroller and ultrasonic sensor. Therefore, the system selects the LDO low-dropout regulator chip

CAT6219-330 to provide a stable supply voltage. The peripheral circuit of the chip is simple, only three capacitors are required to output a stable 3.3V voltage, and the circuit has a fast response time and low output noise and is suitable for use in a battery power supply circuit. The circuit schematic of the voltage regulator circuit is shown in Fig. 3. The capacitor C15 in the circuit is a bypass capacitor, which is used to reduce the output noise of the chip, and C13 and C14 are the filter capacitor stabilization circuit voltage. When the input voltage of the chip is lower than 2.15V, the output is disabled. When the circuit works normally, the power consumption is relatively low, which can meet the power supply requirements of the signal transmitting module[22].

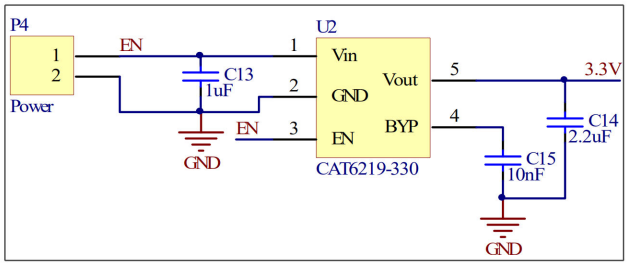

FIGURE 3. Schematic diagram of the transmitter voltage regulator circuit.

The ultrasonic infrared signal transmitting circuit requires a pulse control signal of a certain width to drive. In order to obtain the pulse control signal, the system uses the single-chip microcomputer to generate the required signal through software programming and selects the 8-pin single-chip STC15W204S generated by Hongjing Technology. It has the characteristics of wide voltage, high speed, high reliability, low power consumption and super anti-interference, and the internal integrated high-precision R/C clock can eliminate the external expensive crystal oscillator circuit. The schematic diagram of the circuit generated by the pulse signal is shown in Fig. 4. According to the requirements of the pulse signal, the system uses the MCU timer T0 to time the IO level. Moreover, the system periodically outputs a pulse signal of a certain width on pins P5.4 and P3.3 to control

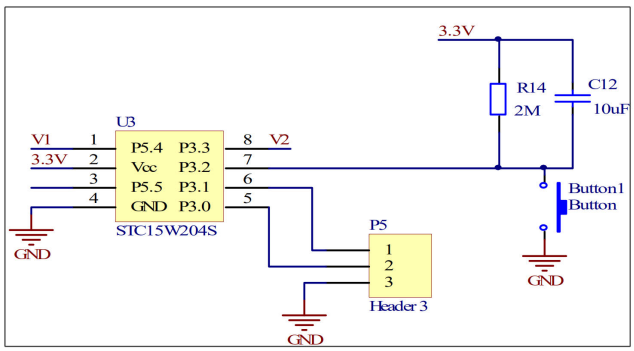

FIGURE 4. Schematic diagram of the circuit generated by the pulse signal.

the signal transmitting circuit and transmit the ultrasonic signal and the infrared signal [23].

Combined with experimental test analysis, the ultrasonic drive circuit selects 300us pulse width control signal, which can meet the ultrasonic signal emission requirements, and the circuit energy consumption is relatively low. The infrared drive circuit uses 200us pulse width control signal to transmit infrared signal. At the same time, the period of the pulse control signal is 20ms, that is, 50 pulse signals are transmitted every second, and the receiving end can complete the processing of the signal, and the selection of this period can also meet the visual requirements of the human eye. The system uses the P5.4 pin of the single-chip STC15W204S to transmit an ultrasonic drive signal with a pulse width of 300us and a period of 20ms and uses the P3.3 pin to transmit an infrared drive signal with a pulse width of 200us and a period of 20ms [24].

The system designed ultrasonic infrared positioning system can realize high-precision positioning of two-dimensional plane. The selection of the ultrasonic emission sensor requires that the two signal receiving ends can effectively receive the ultrasonic signal, so the system selects an 80 KHz piezoelectric film (PVDF) ultrasonic sensor. It is an omnidirectional sensor that emits ultrasonic signals 360° horizontally. The sensor has excellent propagation characteristics and has a low resonant Q value, that is, the sensor's transmitting and receiving performance is superior to the traditional piezoelectric ceramic ultrasonic sensor, which is suitable for planar positioning [25].

For the selection of infrared sensors, an infrared sensor capable of emitting omnidirectionally in the horizontal direction is also required. Since there is no omnidirectional infrared sensor, the system selects four 120-degree emission angle patches of GaAs infrared diodes to be uniformly fixed around the ultrasonic sensor to achieve 360-degree omnidirectional emission of infrared signals. The infrared signal emitted by the gallium arsenide infrared diode has the advantages of high output energy, no redness at all, or only weak red storm. Moreover, the infrared diode has a fast action time, a small transmission delay, and strong anti-interference, so it is suitable as a clock signal of the synchronous system of the system [26].

The signal receiving circuit is an important part of the positioning system, and mainly completes the receiving, processing, and timely extraction of the ultrasonic infrared signal. Therefore, the influence of the receiver on the signal receiving and amplifying performance determines the quality of the signal sent to the signal processing part, which directly affects the extraction of the ultrasonic signal delay and also affects the stability and positioning accuracy of the system. The signal receiving circuit is composed of two infrared receiving circuits, two ultrasonic receiving circuits, a microprocessor and the like. The infrared signal receiving sensor in the receiving circuit selects the ultra-high frequency, high-power photodiode SFH205FA, and its receiving attenuation curve is shown in Fig. 5 [27].

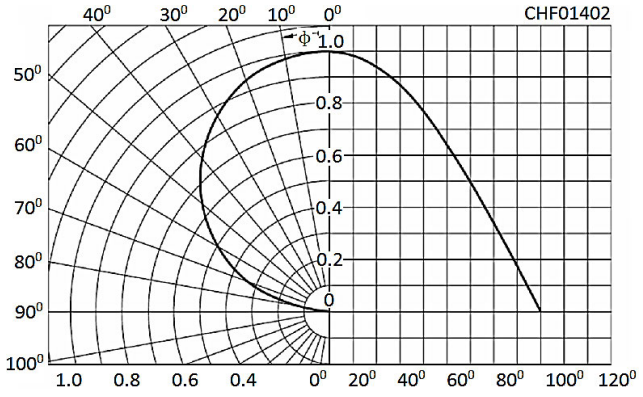

FIGURE 5. Schematic diagram of the circuit generated by the pulse signal.

As can be seen from Fig. 5, the acceptance angle of the infrared receiving tube when the receiving performance is reduced by half is 60°. In order to better receive the infrared signal, the infrared receiving circuit adopts three SFH205FA receiving tubes connected in parallel with each other to realize the receiving of the infrared signal of the entire positioning plane. The ultrasonic signal receiving sensor uses a PVDF piezoelectric film ultrasonic receiving sensor. The reason is that the PVDF ultrasonic sensor has a lower resonant Q value, and the signal rise and decay time are shorter than the conventional piezoelectric crystal ultrasonic sensor at the time of reception, and this characteristic makes the received ultrasonic signal have higher resolution and is suitable for positioning applications. Moreover, the PVDF sensor is an omnidirectional sensor that does not have to consider the sensor angle problem in the circuit [28].

III. EXPERIMENT RESULTS

From September 2017 to August 2018, the ASAI-II grade was randomly selected, and 150 infants who underwent unilateral groin surgery were selected, including 85 males and 66 females. The age is from September to 3 years (median age 1.8 years) and the weight is 8.8-18.2kg. The types of surgery included high ligation of the inguinal hernia sac and high ligation of the sheath, and informed consent was given to the parents before the operation. 150 children who met the inclusion criteria were randomly divided into 3 groups ($n = 50$) according to the digital table method: surgery group II, surgery group II, and surgery group III (referred to as group I, group II, group III). Group I was injected with a small dose of anesthetic under ultrasound guidance, group II was injected with a larger dose of anesthetic under ultrasound guidance, and group III was injected with the same dose of anesthetic with group II using surface anatomy.

When visiting a child before surgery, it is necessary to ban the child from banned solid food and formula for 6 hours, ban drinking for 2 hours, and do not give any medicine before surgery.

After the child enters the operating room, the monitor is connected to monitor the respiratory rate (I), heart rate (HR), electrocardiogram (ECG), blood pressure (BP), pulse oximetry (Sp02), end-tidal carbon dioxide (PETC02), and bispectral index (BIS). All patients were induced by inhalation of 8% sevoflurane. After the consciousness disappeared, the venous access was opened, and the vein was slowly injected with sufentanil 0.2ug/kg. The child's spontaneous breathing is retained, and the jaw is relaxed. After the BIS value is reduced to 60, a proper size mask is placed. Thereafter, the sevoflurane inhalation concentration was adjusted to 2% to 5%, and the appropriate anesthesia depth was maintained, and the BIS value was fluctuated between 40 and 60.The changes of RR and HR were closely observed during the operation. If the RR is lower than 16 bpm, the waveform of PETC02 is higher than 40 mmHg or the waveform is inconsistent, Sp02 $< 95\%$, the oxygen inhalation concentration is increased, and the manual breathing capsule assisted breathing is taken until the spontaneous breathing is cultured. If the HR increase in the child exceeds 10% of the baseline value, the inhaled concentration of sevoflurane in the child is appropriately increased. If the HR is reduced by more than 20% of its base value, atropine is administered at 0.01 mg/kg, and the inhalation concentration of sevoflurane is appropriately reduced. Immediately after the end of the operation, the child stopped inhaling sevoflurane and inhaled 100% pure oxygen to remove residual sevoflurane from the lungs and the laryngeal mask was removed.

After general anesthesia in group I and group II, the child was placed on the operating bed, and the ultrasound probe was applied with a coupling agent. The probe was placed laterally on the lateral side of the umbilicus on the surgical side. After that, the ultrasound is used to identify the tissue structure around the posterior rectus sheath and the rectus abdominis, and the vertical axis of the ultrasound probe is flat on the umbilical cord, and the rectus abdominis is visible from the center of the abdomen near the abdominal wall, and the probe moves slowly from the inside to the outside. On the outside of the rectus abdominis, it can be seen that the multi-layered structure is muscle. From the shallow to the deep, the external oblique muscle, the internal oblique muscle, the transverse abdominis muscle, and the peritoneum. The fascia is highly echoed between the various muscle layers (see Fig. 6).

The inside of the probe was disinfected with 0.5% PVP.I disinfectant. After the towel was placed under the guidance of ultrasound, a 20G puncture needle was used to parallel the long axis of the ultrasound probe at the intersection of the anterior humeral line and the umbilical level to the middle of the transverse abdominis muscle and the intra-abdominal oblique muscle (see Fig. 2). It is clear that the needle tip of the puncture needle is positioned in the fascia layer between the transverse abdominis muscle and the intra-abdominal oblique muscle. The local anesthetic can be injected without pumping blood, and the process of diffusion of the drug solution along the plane of the fascia layer is observed. Group I was injected with 0.25% ropivacaine hydrochloride 0.4 ml/kg and Group II was injected with 0.25% ropivacaine

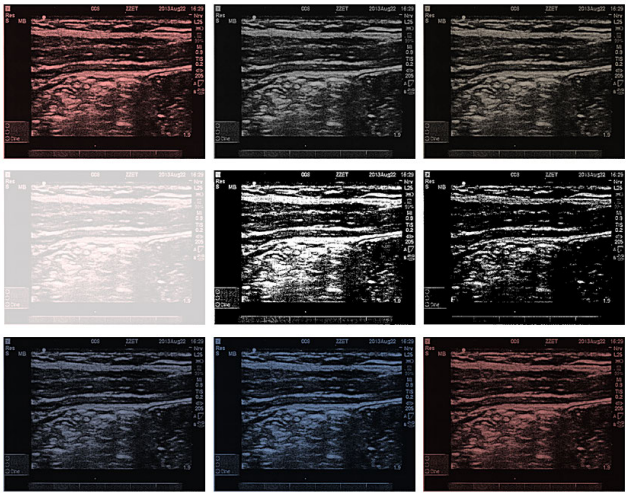

FIGURE 6. Abdominal muscle and fascia anatomical structure under ultrasound.

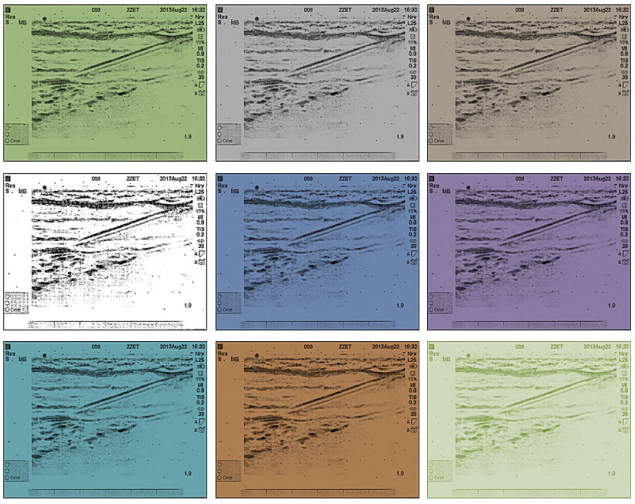

FIGURE 7. Fascia layer when the needle reaches the transverse abdominis muscle under ultrasound.

hydrochloride 0.5 ml/kg by the same method. When injecting the drug, we should closely observe the diffusion range of the drug solution (see Fig. 3). After the injection, the needle is pulled out. All of the nerve block operations in Groups I and II were performed by two senior physicians who were skilled in the application of ultrasound, and the operating time was controlled within 1 minute.

The children in group III were lying on the operating bed, the operator stood on the healthy side of the child, and the latissimus dorsi was touched from front to back along the affected side. In the Petit Triangle, the needle is inserted into the head of the child, and the tip of the needle touches the external oblique muscle. After that, after the needle is inserted into the intra-abdominal oblique muscle and the external oblique muscle fascia, the needle tip enters the plane of the transverse abdominis fascia. After that, 0.25% ropivacaine hydrochloride 0.5 ml/kg was injected, and all the nerve block

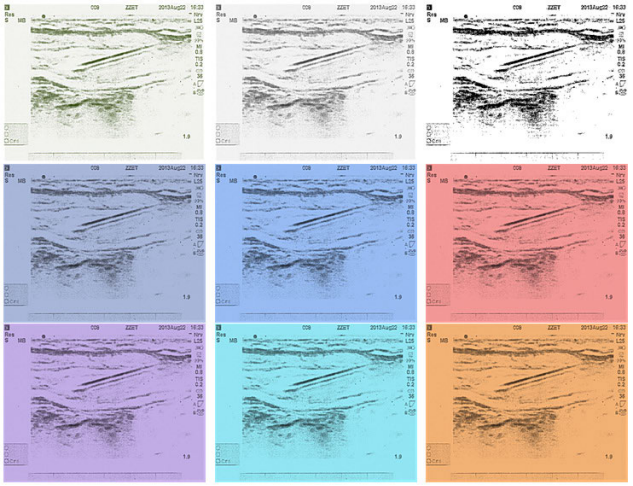

FIGURE 8. "Dough circle sign" formed by drug injection into the transverse abdominis fascia under ultrasound direct vision.

operations were performed by two senior anesthesiologists, and the operation time was controlled within 1 min. The same type of puncture needle was used for each group. The results of the study indicate that ultrasound-guided TAPB is the application of ultrasound imaging techniques to TABB anesthesia, making the TAPB puncture and injection process clear and visible.

IV. ANALYSIS AND DISCUSSON

General anesthesia combined with local nerve block is a commonly used method of anesthesia in clinic. Local nerve block is widely used in various surgical fields because of its simple and easy operation and small influence on the physiological function of patients. In this study, the new long-acting amide local anesthetic ropivacaine hydrochloride was used to perform the transverse abdominis fascia plane block. The mechanism of action of this drug is to block nerve excitation and conduction by inhibiting the sodium channel of nerve cells. The drug has a long-lasting effect, has anesthesia and analgesic effects, and has low cardiotoxicity, and the separation of sensory block and motor block is obvious, and there is peripheral vasoconstriction. Therefore, the drug is especially suitable for anesthesia and analgesia of nerve block. Heart rate is one of the effective indicators for judging the block effect during surgery. In this study, children with group I and group II had insufficient analgesia during operation, which led to an increase in heart rate. In group III, there were 13 patients with insufficient analgesia who needed to increase the inhaled concentration of sevoflurane. There were significantly fewer cases of analgesia in group I and group II than in group III ($P < 0.05$). That is, the ultrasound-guided TABB group was less than the Petit triangulation TAPB group. It can be inferred that the effect of intraoperative analgesia in the ultrasound-targeted group is significantly better than that in the Petit triangulation TAPB when performing the TAPB operation.

Through comparison between the three groups in this study, it was found that the heart rate of group I and group II was significantly lower than that of group III ($P < 0.05$) when the skin was cut and pulled. This indicates that under the strong stimulation of the incision and lifting of the sac/sheathing process, the heart rate of the Petit triangulation group is significantly increased, and the depth of anesthesia is relatively shallow. However, the depth of anesthesia in the ultrasound-targeted group was relatively appropriate, and the hemodynamic fluctuations were small, and the vital signs were stable.

This study found that most of the indicators of the children in each group had the same trend with time, and the heart rate at each time point in the three groups was lower than the heart rate when the child just entered the room. This indicates that the anesthesia depth at this time is deeper than other time points, but it remains in the normal range. The respiratory rate at each time point in the three groups was higher than the respiratory rate at the time of admission, indicating that under anesthesia, the child increased the number of breaths by self-regulation to compensate for the amount of ventilation in the body. PETC02 at T2 and T3 was higher than PETC02 at T1, and the exhaled concentration of sevoflurane at each time point was significantly lower than exhaled concentration of sevoflurane that at the time of initial entry into the room ($P < 0.05$). It indicates that the expiratory phase is prolonged under the anesthesia state at this time, and the ventilation volume is relatively insufficient compared with the physiological state, and the hand-controlled assisted breathing can be performed to supplement the ventilation volume. There was no significant difference in the BIS values between the groups during the operation, indicating that the depth of general anesthesia was similar in each group. The BIS values at the T and T5 time points of each group were significantly higher than those at T2, T3 and T4, suggesting that the depth of anesthesia during surgery was significantly deeper than that at the beginning of anesthesia and when awake. All the indexes of the children in each group were maintained in the normal range, which proved that the method of general anesthesia combined with local anesthesia of TABP was safe and reliable.

Postoperative pain is acute pain that occurs immediately after surgery and generally lasts no more than 7 days. It is characterized by acute nociceptive pain and is the most common and most urgent acute pain in the clinic. If postoperative pain cannot be adequately controlled in the initial state, it may develop into chronic pain with an incidence of 2% to 56%. Moreover, its nature may also translate into neuropathic pain or mixed pain. Pain is a subjective feeling in infants and children, and the child often has unavoidable wound pain after surgery. Many parents think that infants and young children are not sensitive to pain, so children crying after surgery will be mistaken by their parents for hunger, thirst and other reasons, resulting in postoperative pain is often ignored.

V. CONCLUSION

Based on the ultrasound guidance technology, this study automatically locates the anesthesia points, improves the anesthesia efficiency and reduces the damage of the anesthesia to the patient's body. When using the ultrasonic phase angle for positioning, the system requires too much hardware equipment, and high-precision positioning is not allowed. Therefore, this topic selects the ultrasonic arrival time (TOA) to achieve positioning. The method needs to synchronize the transmitting end and the receiving end time, which can be implemented by using radio or infrared rays. Since the wireless transceiver module is not easy to integrate, the latter is selected as a time synchronization signal to achieve high-precision positioning. Through the error analysis of the TOA positioning method used in the positioning system, it can be known that after the wave speed of the ultrasonic signal is compensated by temperature, as long as the measurement accuracy of the left and right ultrasonic delays can be ensured, the positioning accuracy of the system can be theoretically ensured. In order to extract accurate ultrasonic delay, the signal processor designs an ultrasonic signal delay extraction algorithm according to the characteristics of the ultrasonic waveform after acquiring the ultrasonic signal, and accurately determines the ultrasonic arrival time. The results of the study indicate that ultrasound-guided TAPB is the application of ultrasound imaging techniques to TABB anesthesia, making the TAPB puncture and injection process clear and visible.

ACKNOWLEDGMENT

Huanqiu Liu and Tingting Yu designed the research framework and wrote the manuscript, and they have the same contribution.

REFERENCES

[1] Y.-N. Yu, F. Doctor, S.-Z. Fan, and J.-S. Shieh, "An adaptive monitoring scheme for automatic control of anaesthesia in dynamic surgical environments based on bispectral index and blood pressure," *J. Med. Syst.*, vol. 42, no. 5, pp. 95–107, May 2018.

[2] K. Kayashima and K. Imai, "Mispositioning the end of a cuff inflating line in long-axis ultrasound imaging of the pediatric larynx and trachea," *Pediatric Anesthesia*, vol. 28, no. 1, pp. 75–76, Jan. 2018.

[3] S.-C. Kim, I. Gräff, and S. Weber, "A supraclavicular fossa ultrasound window for central venous catheter positioning," *Anesthesia Analgesia*, vol. 124, no. 4, pp. 1374–1375, Apr. 2017.

[4] S. Dong, Z. Yuan, C. Gu, F. Yang, H. Fu, C. Wang, C. Jin, and J. Yu, "Research on intelligent agricultural machinery control platform based on multi-discipline technology integration," *Trans. Chin. Soc. Agricult. Eng.*, vol. 33, no. 8, pp. 1–11, 2017.

[5] E. Smistad, D. H. Iversen, L. Leidig, J. B. Lervik Bakeng, K. F. Johansen, and F. Lindseth, "Automatic segmentation and probe guidance for real-time assistance of ultrasound-guided femoral nerve blocks," *Ultrasound Med. Biol.*, vol. 43, no. 1, pp. 218–226, Jan. 2017.

[6] S. Montazeri, C. Gisinger, M. Eineder, and X. X. Zhu, "Automatic detection and positioning of ground control points using TerraSAR-X multi-aspect acquisitions," *IEEE Trans. Geosci. Remote Sens.*, vol. 56, no. 5, pp. 2613–2632, May 2018.

[7] Y. Tisserand, L. Cuel, and N. Magnenat-Thalmann, "Automatic 3D garment positioning based on surface metric," *Comput. Animation Virtual Worlds*, vol. 28, nos. 3–4, p. e1770, May 2017.

[8] S. Ma, J. Wang, X. Meng, and J. Wang, "A vessel positioning algorithm based on satellite automatic identification system," *J. Electr. Comput. Eng.*, vol. 2017, pp. 1–8, Dec. 2017.
[9] M. Pesteie, V. Lessoway, P. Abolmaesumi, and R. N. Rohling, "Automatic localization of the needle target for ultrasound-guided epidural injections," *IEEE Trans. Med. Imag.*, vol. 37, no. 1, pp. 81–92, Jan. 2018.
[10] C. E. Tatsui, C. N. G. Nascimento, D. Suki, B. Amini, J. Li, A. J. Ghia, J. G. Thomas, R. J. Stafford, L. D. Rhines, J. P. Cata, A. J. Kumar, and G. Rao, "Image guidance based on MRI for spinal interstitial laser thermotherapy: Technical aspects and accuracy," *J. Neurosurgery, Spine*, vol. 26, no. 5, pp. 605–612, May 2017.
[11] J. M. Zimmerman and B. J. Coker, "The nuts and bolts of performing focused cardiovascular ultrasound (FoCUS)," *Anesthesia Analgesia*, vol. 124, no. 3, pp. 753–760, Mar. 2017.
[12] M. C. Parra, K. Washburn, J. R. Brown, M. L. Beach, M. P. Yeager, P. Barr, K. Bonham, K. Lamb, and R. W. Loftus, "Fluoroscopic guidance increases the incidence of thoracic epidural catheter placement within the epidural space: A randomized trial," *Regional Anesthesia Pain Med.*, vol. 42, no. 1, pp. 17–24, 2017.
[13] A. Pasternak, M. Szura, R. Solecki, M. Matyja, A. Szczepanik, and A. Matyja, "Impact of responsive insertion technology (RIT) on reducing discomfort during colonoscopy: Randomized clinical trial," *Surgical Endoscopy*, vol. 31, no. 5, pp. 2247–2254, May 2017.
[14] L. E. Imbellon, M. A. Gouveia, and G. B. de Morais Filho, "Comparison of the effects of four subdoses of dextroketamine to reduce pain during posterior brachial plexus block: A randomized double blind study," *Anesthesia, Essays Res.*, vol. 11, no. 2, pp. 345–349, 2017.
[15] K. S. Savitha, R. Dhanpal, and M. S. Vikram, "Hemodynamic responses at intubation, change of position, and skin incision: A comparison of multimodal analgesia with conventional analgesic regime," *Anesthesia, Essays Res.*, vol. 11, no. 2, pp. 314–320, 2017.
[16] I. A. Bambaren, F. Dominguez, M. E. E. Martin, and S. Domínguez, "Suppl-6, M4: Anesthesia and analgesia in the patient with an unstable shoulder," *Open Orthopaedics J.*, vol. 2017, no. 11, pp. 848–860, 2017.
[17] K. H. Kook, S. A. Chung, S. Park, and D. H. Kim, "Use of the bispectral index to predict eye position of children during general anesthesia," *Korean J. Ophthalmol.*, vol. 32, no. 3, pp. 234–240, 2018.
[18] U. Gurunathan, S. M. Kunju, K. E. Hay, and S. van Alphen, "Usefulness of a visual aid in achieving optimal positioning for spinal anesthesia: A randomized trial," *BMC Anesthesiol.*, vol. 18, no. 1, pp. 1–11, Dec. 2018.
[19] K. Hirooka, K. Ukegawa, E. Nitta, N. Ueda, Y. Hayashida, H. Hirama, R. Taoka, Y. Sakura, M. Yamasaki, H. Tsunemori, M. Sugimoto, and Y. Kakehi, "The effect of steep Trendelenburg positioning on retinal structure and function during robotic-assisted laparoscopic procedures," *J. Ophthalmol.*, vol. 2018, pp. 1–8, Jun. 2018.
[20] V. Z. Kovari and L. Horvath, "Surgical management of cauda syndrome in third trimester of pregnancy focusing on spinal anesthesia and right lateral positioning during surgery as possible practices," *Eur. Spine J.*, vol. 27, no. 3, pp. 483–488, Jul. 2018.
[21] N. Lockwood, J. Parker, C. Wilson, and P. Frankel, "Optimal anesthetic regime for motionless three-dimensional image acquisition during longitudinal studies of adult nonpigmented zebrafish," *Zebrafish*, vol. 14, no. 2, pp. 133–139, Apr. 2017.
[22] D. Krzemiński, M. Kamiński, A. Marchewka, and M. Bola, "Breakdown of long-range temporal correlations in brain oscillations during general anesthesia," *NeuroImage*, vol. 159, pp. 146–158, Oct. 2017.
[23] K. V. Nourski, M. I. Banks, M. Steinschneider, A. E. Rhone, H. Kawasaki, R. N. Mueller, M. M. Todd, and M. A. Howard, "Electrocorticographic delineation of human auditory cortical fields based on effects of propofol anesthesia," *NeuroImage*, vol. 152, pp. 78–93, May 2017.
[24] L. K. Borg, T. K. Harrison, A. Kou, E. R. Mariano, A. D. Udani, T. E. Kim, C. Shum, S. K. Howard, and ADAPT (Anesthesiology-Directed Advanced Procedural Training) Research Group, "Preliminary experience using eye-tracking technology to differentiate novice and expert image interpretation for ultrasound-guided regional anesthesia," *J. Ultrasound Med.*, vol. 37, no. 2, pp. 329–336, 2018.
[25] V. Ratner, Y. Gao, H. Lee, R. Elkin, M. Nedergaard, H. Benveniste, and A. Tannenbaum, "Cerebrospinal and interstitial fluid transport via the glymphatic pathway modeled by optimal mass transport," *NeuroImage*, vol. 152, pp. 530–537, May 2017.
[26] Z. Liu, L. Zhao, Q. Jia, X. Yang, S. J. Liang, and W. He, "Chest computed tomography image for accurately predicting the optimal insertion depth of left-sided double-lumen tube," *J. Cardiothoracic Vascular Anesthesia*, vol. 32, no. 2, pp. 855–859, Apr. 2018.
[27] G. Konig, J. H. Waters, E. Hsieh, B. Philip, V. Ting, G. Abbi, M. Javidroozi, G. W. Tully, and G. Adams, "*In vitro* evaluation of a novel image processing device to estimate surgical blood loss in suction canisters," *Anesthesia Analgesia*, vol. 126, no. 2, pp. 621–629, 2017.
[28] F. Zhao, L. Li, W. Zhou, D. Shi, Y. Fan, and L. Ma, "Correlative factors' analysis of postural-related ocular cyclotorsion with image-guided system," *Japanese J. Ophthalmol.*, vol. 62, no. 2, pp. 37–242, 2018.

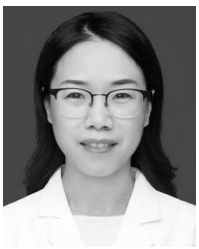

HUANQIU LIU received the Ph.D. degree in five-year clinical medicine system from Jilin University. She is currently an Associate Chief Physician of the Anesthesiology Department, The First Hospital of Jilin University. She is a Master Tutor and Master of Medicine with Jilin University. She studied anesthesia for liver transplantation surgery with the Zhongshan Hospital Affiliated to Fudan University, Shanghai, studied ultrasound-guided nerve block technology with the Beijing Jishuitan Hospital and Shanghai Sixth Hospital successively, took the lead in leading department personnel to carry out ultrasound-guided regional nerve block technology, and popularized the technology in her department. In 2019, she visited the Vickers Forest Medical Center, USA, focusing on the perioperative management of trauma patients and nerve block technology guided by ultrasound combined with nerve stimulator.

FUZHE MA was born in May 1983. He is a Deputy Chief Physician of the Nephrology Department, The First Hospital of Jilin University, and the Doctor of Clinical Medicine with Jilin University. He has published 11 SCI articles and presided two scientific research projects. He is good at difficult blood purification pathway establishment surgery, as well as CRRT, and other complex hemodialysis techniques. His main social part-time jobs: a member of the Nephrology Branch of Jilin Society of Integrated Traditional Chinese and Western Medicine, the Jilin Home Pension Association, and the Nephrology Branch of Changchun Society of Integrated Traditional Chinese and Western Medicine.

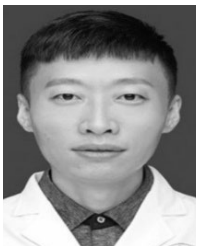

JI LI is currently a Deputy Chief Physician of the Department of Anesthesiology, The First Hospital of Jilin University and the Doctor of clinical medicine of Seven-Year Clinical Medicine System with Jilin University. He studied anesthesia for liver transplantation with Zhongshan Hospital Affiliated to Fudan University in Shanghai. As the first author or correspondent, he has published eight articles in SCI journals.

TINGTING YU received the Ph.D. degree in seven-year clinical medicine program from Jilin University, with research interests in head and neck oncology and voice medicine. She is currently an Attending Surgeon, a Master of medicine, the Head and Neck of Otolaryngology with The First Hospital of Jilin University. She is a member of the Voice Expert Committee of the Chinese Otolaryngology Professional Committee of Integrated Traditional Chinese and Western Medicine, and a member of the First Sleep Disorders Professional Committee of the Jilin Institute of Integrated Traditional Chinese and Western Medicine. From 2015 to 2016, she studied at the Karolinska Medical College, Sweden.

XINBAI LI is currently a Deputy Chief Physician, a Master's Tutor, and the Doctor of clinical medicine. She studied with the Wuxi People's Hospital, Shanghai Sixth Hospital, and Beijing Chaoyang Hospital. She has published more than 20 articles, SCI included four articles. In her capacity as the Editor-in-Chief, she published one treatise. Her research interests include perioperative pain management and multimodal analgesia.